FEATURE ARTICLE

ChemComm
www.rsc.org/chemcomm

Solid-state electroluminescent devices based on transition metal complexes

Jason Slinker,[a] Dan Bernards,[a] Paul L. Houston,[b] Héctor D. Abruña,[b] Stefan Bernhard[c] and George G. Malliaras*[a]

[a] *Department of Materials Science and Engineering, Cornell University, Ithaca, NY 14853, USA. E-mail: george@ccmr.cornell.edu*

[b] *Department of Chemistry and Chemical Biology, Cornell University, Ithaca, NY 14853, USA*

[c] *Department of Chemistry, Princeton University, Princeton, NJ 08544, USA*

Received (in Cambridge, UK) 17th April 2003, Accepted 3rd June 2003
First published as an Advance Article on the web 17th July 2003

Transition metal complexes have emerged as promising candidates for applications in solid-state electroluminescent devices. These materials serve as multifunctional chromophores, into which electrons and holes can be injected, migrate and recombine to produce light emission. Their device characteristics are dominated by the presence of mobile ions that redistribute under an applied field and assist charge injection. As a result, an efficiency of 10 lm/W—among the highest efficiencies reported in a single layer electroluminescent device—was recently demonstrated. In this article we review the history of electroluminescence in transition metal complexes and discuss the issues that need to be addressed for these materials to succeed in display and lighting applications.

Introduction

Transition metal complexes, such as ruthenium tris-bipyridine $[Ru(bpy)_3]^{2+}$, shown in Fig. 1, have been the subject of extensive electrochemical and spectroscopic studies. The interest in this class of materials stems from the fact that they exhibit multiple stable oxidation states and have attractive excited state properties.[1] The observation of light emission in electrochemical cells[2] (called electrogenerated chemiluminescence) or by electron transfer processes, in general, has prompted a great deal of studies of their optoelectronic properties in solution.

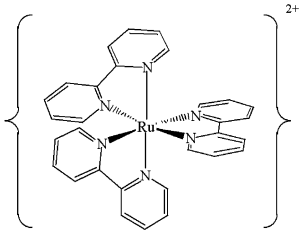

Fig. 1 Chemical structure of $[Ru(bpy)_3]^{2+}$.

In a parallel effort, organic light emitting diodes (OLEDs) are being developed for applications in flat panel displays and lighting.[3] In the simplest configuration, an OLED consists of a single layer of an organic semiconductor sandwiched between two metal electrodes, the anode and the cathode (in forward bias, the latter is biased negative with respect to the former). Under the application of a forward bias, holes are injected from the anode into the highest occupied molecular orbital (HOMO) of the organic layer and migrate towards the cathode. In a similar fashion, electrons injected from the cathode into the lowest unoccupied molecular orbital (LUMO) of the organic migrate towards the anode. When a hole and an electron meet in the bulk of the organic layer, they may combine to form an exciton. A fraction of these excitons recombine radiatively, giving rise to light emission. The basic requirements from the organic semiconductor are the ability to transport both electrons and holes, and a high luminescence efficiency.

Transition metal complexes satisfy these requirements. Their excellent stability in multiple redox states indicates that electronic carriers can be readily injected and transported in these materials. Their luminescence efficiency can be high, evident from the fact that these materials have been used as tracer dyes in sensor applications. In $[Ru(bpy)_3]^{2+}$, which is a model compound for this class of materials, the highest occupied molecular orbital (HOMO) is the t_{2g} orbital of the metal, while the lowest unoccupied molecular orbital (LUMO) is the π^* orbitals of the ligands. Electron transport in a $[Ru(bpy)_3]^{2+}$ film is described as a series of redox reactions involving electron hopping in the LUMO of the molecules. Similarly, hole transport takes place through the HOMO. Light emission arises from the $\pi^* \rightarrow t_{2g}$ ligand to metal transition.[4]

In addition to satisfying the basic requirements of electronic carrier transport and emission, transition metal complexes feature ionic conductivity. For example, $[Ru(bpy)_3]^{2+}$ carries a net 2+ charge, which is compensated by two counter ions such as PF_6^- or ClO_4^-. In a film, these counter ions are mobile at room temperature, and dominate the device characteristics. In this respect, electroluminescent devices made from transition metal complexes are similar to the so-called light-emitting electrochemical cells (LECs), fabricated by dispersing salts into organic semiconductors.[5] Transition metal complexes, however, are more stable than the dispersions used in LECs. Since the ions are an integral part of their structure, they do not suffer from phase separation.

The first solid-state electroluminescent device from a transition metal complex was reported in 1996 by the MIT group.[6] Since then, tremendous progress has been achieved in the performance of these devices,[7–29] which today is close to that of the best organic light-emitting diodes. As with every new class of electroluminescent materials, questions arise regarding (i) the ultimate limits of their efficiency, (ii) their response time, (iii) the availability of multiple colours, as well as (iv) their lifetime in devices. We begin this article by discussing the device operation mechanism as we understand it today. We shall then address these questions in four separate sections. One has to keep in mind that the field of transition metal complex electroluminescence is still in its early stages, and the relationships among chemical structure, processing conditions and device performance are still under investigation. Most of the studies carried out thus far have been exploratory in nature and have not rigorously pursued the link between materials parameters and device performance. Keeping this in mind, we will follow the brief history of the field and outline the steps that led to today's high-performance devices. We end by discussing

DOI: 10.1039/b304265k

 This journal is © The Royal Society of Chemistry 2003

the challenges that remain to be addressed in order to ensure the commercial viability of these materials in electroluminescent devices.

We wish to note that this article deals only with solid-state devices, where the transition metal complexes were used as multifunctional chromophores. Hence, we do not include works where transition metal complexes were utilized as luminescent dopants in organic light emitting diodes, nor do we discuss solution-based electroluminescent devices (so-called electrogenerated chemiluminescent devices).

Operation mechanism

In Fig. 2, typical characteristics of a transition metal complex-based electroluminescent device are shown.[18] The device was

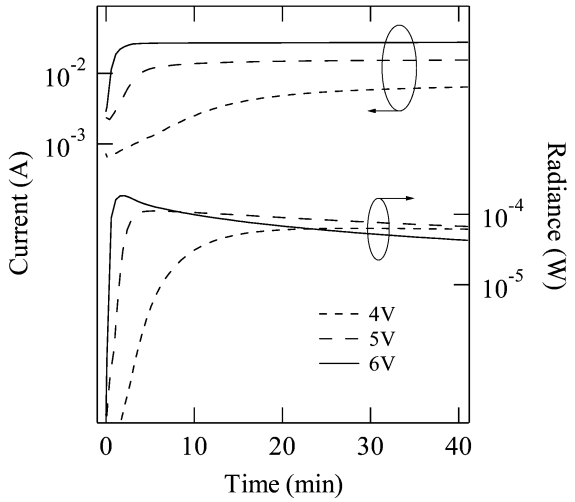

Fig. 2 Characteristics of ITO/$[Os(bpy)_2L]^{2+}(PF_6^-)_2$/Au devices.

fabricated by spin-coating a thin (*ca*. 100 nm thick) film of the complex $[Os(bpy)_2L]^{2+}(PF_6^-)_2$, where L is *cis*-1,2-bis(diphenyl phosphino)ethylene, on to indium tin oxide (ITO)-covered glass and evaporating a gold top electrode. In contrast to organic light-emitting diodes, where the current and radiance respond almost instantaneously to an applied voltage, a voltage-dependent lag time is observed. The current in Fig. 2 increases slowly to a steady-state value, with a characteristic time that decreases with applied voltage. The radiance initially follows the current, but then decays at a rate that increases with voltage.

These characteristics can be understood on the basis of the interplay between electronic and ionic charges.[30] Upon application of a forward bias, the PF_6^- counter ions drift towards the anode (ITO), where they accumulate and cause a lowering of the barrier for hole injection. Holes are concomitantly injected in the HOMO of $[Os(bpy)_2L]^{2+}$, which corresponds to the removal of an electron from the t_{2g} orbital of Os and the production of $[Os(bpy)_2L]^{3+}$. At the same time, the presence of uncompensated $[Os(bpy)_2L]^{2+}$ ions in the neighbourhood of the cathode enhances electron injection, which takes place in the π^* orbital of the ligand and results in the formation of $[Os(bpy)_2L]^{+}$. As more and more PF_6^- ions accumulate near the anode, hole and electron injection are enhanced, giving rise to the increase in current observed in Fig. 2. A steady-state is reached when the PF_6^- ions attain their equilibrium distribution near the anode, dictated by the applied voltage and the coulombic interactions with the ionic and electronic charges in the device. In the meantime, injected electrons and holes migrate towards opposite electrodes. Emission results from the electron transfer recombination of $[Os(bpy)_2L]^{3+}$ and $[Os(bpy)_2L]^{+}$, which produces the excited state $[Os(bpy)_2L]^{2+*}$ of the complex. A higher applied voltage speeds up the accumulation of the PF_6^- ions at the anode, giving rise to a faster device turn-on (Fig. 2).

One important figure-of-merit of an electroluminescent device is its (external) quantum efficiency (η_Q), which is the ratio of emitted photons per injected electron. It is given by:[3]

$$\eta_Q = b \cdot \phi \cdot q \quad (1)$$

where b is the fraction of injected electrons that combine with holes to form excitons, ϕ is the fraction of excitons that recombine radiatively to produce a photon, and q is the fraction of photons that escape waveguiding and propagate outside the device. The first term, b, is determined by the magnitude and the balance between the electron and hole currents. The second term, ϕ, is equal to the photoluminescence yield in the film. Contrary to organic semiconductors, in which emission arises almost exclusively from the decay of singlet excitons, the strong spin-orbit coupling in transition metal complexes effectively converts all excitons into triplets,[4] which decay radiatively with a yield ϕ. Finally, the third term, q, depends on the refractive indices, the absorption coefficients and the roughness of the various layers.

Ion densities in these complexes are of the order of 10^{21} cm^{-3}. At such high densities, the potential drop caused by accumulation of PF_6^- ions near the anode (and the subsequent depletion near the cathode) can be large enough to decrease the barriers for charge injection to such an extent that the contacts become ohmic.[30] As a result, every injected electron combines with a hole to form an exciton (b = 1)[31] and the device quantum efficiency is determined by the photoluminescence yield of the complex. In addition, the turn-on voltage (lowest voltage at which light is emitted) can be as low as the HOMO/LUMO gap. This is an advantage compared to OLEDs, which are usually limited by charge injection and exhibit larger turn-on voltages. The penalties associated with the existence of the ionic space charge are the comparatively long turn-on time and the absence of rectification.

At present, our understanding of the device operation mechanism remains rather qualitative. Some early modelling work[7,21,32] as well as some experiments[19,27,32,33] have been performed to address issues such as the distribution of the electric field inside the device and the spatial extent of the recombination zone. As a first step towards achieving a quantitative understanding, accurate determination of basic device parameters, such as the barriers for charge injection and the carrier mobilities, is needed.

Efficiency

The quantum efficiency is the figure-of-merit that is most frequently used to benchmark electroluminescent device performance. In Fig. 3, the evolution of the quantum efficiency of transition metal complex-based devices is shown as a function of time.[6–29] The dramatic increase achieved in just a few years came as a result of improved understanding of how the chemical structure of the complexes and their processing into thin films affect device performance. In this section, we discuss the various materials, processing techniques and device geometries that have been used in transition metal complex-based devices.

The first solid-state electroluminescent device from a transition metal complex was reported by Lee *et al.*,[6] who used a ruthenium poly-pyridyl complex. By incorporating sulfonate groups at the *para*-positions of the complex's 4,7-diphenyl-1,10-phenanthroline ligands, they rendered the molecule soluble in water, allowing for spin coating and layer-by-layer processing techniques. Films were deposited by both methods on ITO-covered glass, followed by evaporation of aluminium

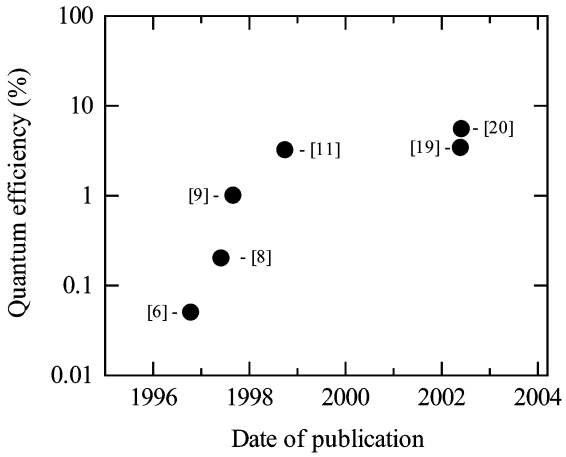

Fig. 3 Evolution of the record quantum efficiency of electroluminescent devices from transition metal complexes. The appropriate reference is indicated next to each datum point.

electrodes, yielding sandwich-type devices. The quantum efficiencies of these devices were relatively low, near 0.005%. Introduction of the conjugated polymer poly(*p*-phenylene vinylene) between the ITO and the complex was found to increase the device efficiency to 0.05%.

The effect of ionic conductivity was explored by Maness *et al.*[7] They reported on an electroluminescent device from a polymeric ruthenium complex, poly[$Ru(vbpy)_3$]$^{2+}$, where vbpy is 4-vinyl-4′-methyl-2,2′-bipyridine, and the PF_6^- counter ion. Films of this material were prepared on Pt interdigitated electrodes (planar-type devices) in either a solvent-swollen state, where the material was ionically conducting, or in a dry state. For the latter, the devices were prepared in the solvent-swollen state, allowed to reach equilibrium under an applied voltage, dried, and cooled to 0 °C to freeze-in the distribution of counter ions. These devices exhibited diode-like characteristics, consistent with the presence of a built-in potential in the ruthenium film. In contrast, the solvent-swollen devices exhibited no rectification. Quantum efficiencies of 0.025% and 0.03% were measured in devices with solvent-swollen and dry films, respectively.

The same group used a highly viscous molten salt of a ruthenium tris-bipyridine derivative to fabricate devices on interdigitated Pt electrodes.[8] A quantum efficiency of 0.2% was measured at room temperature, where the devices did not show any rectification. Cooling the devices down to −20 °C while maintaining the applied voltage allowed them to freeze-in the distribution of counter ions. These devices exhibited a rectification ratio of 100.

A polyester with a ruthenium complex incorporated in the main chain was investigated by Lee *et al.*[9] and Wu *et al.*[11] Devices were fabricated both by spin coating the polymer on ITO-coated glass and by a layer-by-layer deposition, followed by evaporation of aluminium top contacts. While the quantum efficiencies of the best spin-coated devices were only 0.08%, the layer-by-layer devices exhibited efficiencies of the order of 1% (and, in some devices, as high as 3.2%). As numerous differences exist between the local environment in a uniform film (spin-coating) and a stratified one (layer-by-layer deposition), it was difficult to pinpoint the reasons for the increased efficiency in the stratified structures.

Also considering a ruthenium polyester were Elliott *et al.*[10] Their sandwich-configuration devices with this active layer yielded quantum efficiencies between 0.06% and 0.92%. Of note was the fabrication technique used in these devices. The top contact was formed by placing a gold mesh into a drop-cast, monomeric film, followed by polymerization of the polyester.

Gong *et al.*[12] were the first to make devices from a transition metal complex using a metal centre other than ruthenium. They reported electroluminescence in devices based on rhenium complexes blended in polycarbonate, as well as devices based on ruthenium complexes blended in poly(vinyl alcohol). The quantum efficiencies of these devices were estimated to be on the order of 0.1%. It should be noted that the Re compound carries no net charge, therefore it exhibited device characteristics typical of an OLED.

Lyons *et al.*[13] investigated the addition of a solid electrolyte in devices from ruthenium complexes. For that, they utilized the ion conducting polymer poly(ethylene oxide) (PEO) and the salt lithium triflate ($LiCF_3SO_3$). Sandwich-type devices, in which a ruthenium complex was blended with PEO, exhibited a maximum quantum efficiency of 0.02% when a 10:1 molar ratio of PEO monomer units to ruthenium complex was used. Preserving this ratio and adding lithium triflate (20:1 molar ratio of PEO repeat unit to salt), these devices displayed similar efficiencies. Various cathode metals such as Al, Au, Ag and Pt gave devices with a similar turn-on voltage, indicating that the ionic space charge was enough to enhance electron injection and make it independent of the electrode work function.

Handy *et al.*[14] demonstrated that high efficiency devices could be realized by a single-layer, spin-coated film of a low molecular weight ruthenium complex. In particular, they reported efficiencies as high as 1% for a hydroxy-methylated version of $[Ru(bpy)_3]^{2+}(PF_6^-)_2$. This particular work revealed that device efficiencies varied somewhat with modification of the bipyridine ligands. Furthermore, it was reported that acid-etching the ITO electrode prior to device fabrication could enhance the efficiency.

Continuing previous work involving layer-by-layer techniques of processing polyester ruthenium complex films, Wu *et al.*[15] systematically varied both the thickness and concentration of layers of polyester and poly(acrylic acid) (PAA). By changing the pH of the ruthenium polyester and PAA solutions during the deposition process, both the overall thickness of the devices and the relative ratio of the polyester to PAA was varied. The variation of the composition allowed the systematic modification of the site-to-site distance of the ruthenium complexes, which influences self-quenching effects and electronic mobility in the devices. By optimising thickness and composition, quantum efficiencies as high as 3% were realized. By simply changing the thickness of these films at the optimal composition, the efficiency varied from 0.2% at 90 nm to 2% at 200 nm active layer thickness. The turn-on voltage was found to be a function of the number of polyester/PAA bilayers present, with 3 and 5 V turn-on voltages for 15 and 35 bilayer devices, respectively. This was attributed to the high bulk resistance of the multilayer films. It was shown that the order of voltage sweeping, whether from forward bias to reverse or reverse bias to forward, influenced the symmetry of the current *vs.* voltage and radiance *vs*. voltage characteristics. Furthermore, by changing the composition of the multilayers, devices that exhibited light emission preferentially in either the forward or reverse bias operation were fabricated.

Gao and Bard[16] reported on sandwich-type devices based on $[Ru(bpy)_3]^{2+}$ salts with a novel liquid metal electrode. The devices were fabricated by spin-coating the organic onto ITO, followed by printing of a gallium:indium eutectic contact. In addition to a new cathode electrode, the use of a new counter ion, ClO_4^-, was also reported. At 3V forward bias, ITO/$[Ru(bpy)_3]^{2+}(ClO_4^-)_2$/Ga:In devices exhibited quantum efficiencies ranging from 0.4 to 1.8%. Under reverse bias, the radiance was approximately five orders of magnitude less. Inclusion of an aromatic hole transport layer between the ITO and the ruthenium complex did not have a significant effect on device performance.

Extending the idea of polymer blending to $[Ru(bpy)_3]^{2+}(PF_6^-)_2$ films, Rudmann and Rubner[17] mixed this complex with poly(methyl methacrylate) (PMMA), polycarbonate (PC), and polystyrene (PS). In the case of PMMA, devices with varied volume content of PMMA dispersed in $[Ru(bpy)_3]^{2+}(PF_6^-)_2$ were fabricated. A maximum quantum efficiency of 3% was measured at a PMMA concentration of approximately 25% vol., in sandwich-type devices using Ag cathodes. Devices with Ag cathodes consistently performed with higher efficiencies (2.5–3.0%) than those with Al contacts (2.0–2.5%), and this disparity was believed to be due to the greater tendency for electrochemical degradation of the latter metal. In addition, devices were tested using a pulsed voltage drive consisting of the superposition of an ac and a dc voltage. Under such driving conditions, the devices showed improved efficiencies over dc driving. It was postulated that this improvement might be because of the additional time given for the excited states to relax back to the ground state, reducing overpopulation of the triplet excited states.

Electroluminescence in complexes of osmium were reported by Bernhard *et al.*.[18] Devices based on $[Os(bpy)_2L]^{2+}(PF_6^-)_2$, where L is *cis*-1,2-bis(diphenyl phosphino)ethylene, were made using ITO and Au electrodes and exhibited a quantum efficiency of the order of 1%. The efficiency was found to increase with thickness and decrease with increasing voltage. The former was attributed to quenching of emission near a contact, while the latter to degradation.

A single-crystal device based on a ruthenium complex was reported by Liu and Bard.[19] The device was made by repeatedly injecting a nearly saturated solution of $[Ru(bpy)_3]^{2+}(ClO_4^-)_2$ in acetonitrile between two ITO slides separated by 1 μm, followed by evaporation of the solvent. The resulting device yielded a quantum efficiency of 3.4%. In addition, it exhibited a turn-on voltage similar to that in devices made from thinner, spin-coated films, clearly demonstrating that ions dominate the device performance. Despite the symmetric current *vs.* voltage characteristics, the radiance was asymmetric. This was attributed to asymmetric self-absorption of the emitted light, due to the fact that emission takes place closer to one of the electrodes. The latter is true when electrons and holes have different mobilities.[30]

Furthering their study of ruthenium complexes and polymer blends, Rudmann *et al.*[20] investigated blends of $[Ru(bpy)_3]^{2+}$ and two of its derivatives in PMMA. Various counter ions (PF_6^-, ClO_4^-, and BF_4^-) were used in blends that contained about 25% vol. PMMA. All films reported produced devices with quantum efficiencies in excess of 2.5% under dc driving, with one of the complexes yielding an efficiency of 4.8%. Under pulsed driving, the efficiency increased by about 20%, with the dinonyl-substituted complex exhibiting a 5.5% efficiency, which remains the highest reported quantum efficiency for a transition metal complex-based device to date.

Gao and Bard[23] investigated the influence of electrode conductivity on the characteristics of $[Ru(bpy)_3]^{2+}(ClO_4^-)_2$ devices with ITO and Ga:In contacts. Using ITO with sheet resistance of 100 Ω/□ and 10 Ω/□ did not result in any difference in the quantum efficiency. However, the current and the radiance were significantly greater in the devices with the low resistivity ITO. Using ITO that was heavily doped with In yielded even greater current and radiance, as did applying a 10 nm gold film over the ITO electrode. In addition to the Ga:In alloy contact mentioned above, Ga:Sn and Bi:In:Pt:Sn liquid contacts were reported to give device characteristics similar to Ga:In. Furthermore, the fabrication of functional devices with a printed Hg cathode were demonstrated.

Bernhard *et al.*[24] explored devices of $[Ru(bpy)_3]^{2+}(PF_6^-)_2$ and complexes with the bpy ligand modified with various aliphatic side chains at the 4 and 4′ positions. ITO and Au electrodes were used as the anode and cathode respectively in sandwich-type devices. The devices were found to exhibit the same current and radiance regardless of the direction of the applied field (Fig. 4), indicating that both contacts were ohmic

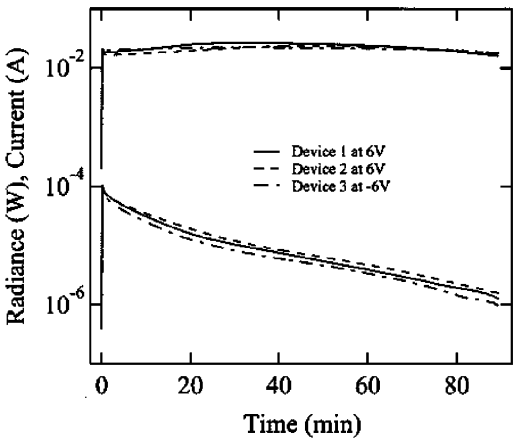

Fig. 4 Temporal evolution of the current (top set of curves) and the radiance (bottom set of curves) of ITO/$[Ru(bpy)_3]^{2+}(PF_6^-)_2$/Au devices at forward and reverse bias, indicating no rectification. From Ref. 24.

for both electron and hole injection. This allowed an estimate of the photoluminescence efficiency of the films. Comparison with the photoluminscence yield of the complexes in solution indicated that self-quenching of the luminescence was small, and it was minimized with di-*n*-pentyl and di-*tert*-butyl (dtb) side chains. Among these compounds, a maximum quantum efficiency of 0.75% was reported for $[Ru(dtb\text{-}bpy)_3]^{2+}(PF_6^-)_2$ devices.

Leprêtre *et al.*[25] investigated the addition of lithium salt/crown ether solid electrolytes in sandwich-type devices of a binuclear ruthenium complex. The salts, lithium triflate or lithium trifluoromethylsulfonyl-imide (Li-TFSI), and the ether 18-crown-6, mixed at a 0.5 molar ratio, were added to the binuclear ruthenium complex. Below 33% wt. of salt/crown ether in the ruthenium complex, no radiance was observed. However, at higher concentrations the devices functioned at 0.02% quantum efficiency regardless of the amount of electrolyte. The radiance was maximal for 75% wt of salt/crown ether. Devices with the Li-TFSI salt showed improved efficiencies over those with lithium triflate. This improvement was attributed to the larger charge delocalization on this anion, which results in a salt with a higher conductivity. Finally, it was reported that the insertion of a conducting polymer layer between the ITO electrode and the ruthenium layer did not significantly change the device efficiency.

Recently, Slinker *et al.*[26] reported on the first device based on an iridium metal complex, namely $[Ir(ppy)_2(dtb\text{-}bpy)]^+(PF_6^-)$, where ppy is phenyl pyridine and dtb-bpy is 4,4′-di-*tert*-butyl-2,2′-dipyridyl (dtb-bpy). Devices were fabricated in a sandwich structure using ITO and Au electrodes and yielded quantum efficiencies of 5% under reverse bias operation at 3V (with the ITO biased negatively). The efficiency was an order of magnitude lower under a forward bias of 3V. The difference was attributed to asymmetric injection—it was suggested that the ionic space charge was not enough to make the contacts ohmic in these devices. Under reverse bias, a power efficiency of 10 lm/W was reported, which is among the highest power efficiencies reported in a single layer electroluminescent device.

The effect of moisture exposure on device efficiency was investigated by Kalyuzhny *et al.*[27] using $[Ru(bpy)_3]^{2+}(BF_4^-)_2$ films. Devices were prepared under an inert atmosphere, then tested either in air or in a dry box for comparison. The maximum quantum efficiencies of devices tested in air were found to be

about two times higher than those for devices tested in the dry box. This was attributed to the fact that water or moisture serves to balance charge carrier injection, at least in the initial stages of operation.

Lee *et al.*[28] investigated the influence of the thickness of a $[Ru(bpy)_3]^{2+}(PF_6^-)_2$ layer on the quantum efficiency in sandwich-type devices with ITO and Au electrodes. A decrease from 1% to less than 0.01% was observed when the thickness of the ruthenium film varied from 192 to 46 nm. The decrease was monotonic, indicating the absence of strong microcavity effects. Spectroscopic measurements indicated that the yield of photoluminescence of $[Ru(bpy)_3]^{2+}(PF_6^-)_2$ films on quartz substrates exhibits only a small variation with thickness, from 2.2% in 200 nm thick films to 1.8% in 17 nm thick films. The large decrease of the quantum efficiency was therefore attributed to quenching of excitons near the electrodes and to triplet-triplet annihilation, which is more pronounced in thinner devices due to the higher current densities.

Barron *et al.*[29] reported on devices based on polyamidoamine dendrimers containing pendant $[Ru(bpy)_3]^{2+}$ groups, sandwiched between ITO and Au electrodes. The quantum efficiency showed a monotonic decrease with dendrimer generation, which was attributed to a decrease in the yield of photoluminescence with dendrimer generation. The latter trend was also observed in solutions of these materials. By comparing the yield of photoluminescence in film and in solution, the degree of self-quenching was extracted for these materials.

Turn-on time

In this section we discuss the influence of materials processing and device conditioning on the turn-on time. The latter is loosely defined as the time it takes to reach the peak radiance and reflects the speed at which these devices can be operated.

The first mention of a turn-on time was by Lee *et al.*[6] in a low molecular weight ruthenium poly-pyridyl complex. A "charging" effect was noted, where devices took 30 s to 2 min to reach 90% of their maximum output. The turn-on voltages ranged from 2.5–3.5 V regardless of film thickness, indicating pronounced ionic space charge effects.

Manness *et al.*[7,8] investigated devices where the distribution of counter ions was frozen-in while the devices were operating. This was achieved by first drying and then cooling solvent-swollen polymeric ruthenium films, and by cooling low molecular weight ruthenium complexes. These devices exhibited nearly instantaneous turn-on, and showed similar quantum efficiencies as in the original state, in which the ions were mobile. Sustained reverse biasing, however, resulted in the breakdown of the frozen concentration gradients and the improvement in the turn-on time for these devices was reduced. At elevated temperatures, fast reversal of steady-state concentration gradients upon reversing bias was attributed to counter ion redistribution times much closer to electron hopping times.

Device conditioning to alter the turn-on time was also explored by Elliott *et al.*[10] in a ruthenium polyester that was polymerised while the device was operated. By pre-biasing, removing the voltage for 5 minutes and then reapplying a voltage, the devices took only 2 minutes to reach their steady-state—a fairly short time for a polymeric material. This was attributed to the *in-situ* polymerisation, which helped lock-in, at least partially, the counter ion concentration gradient.

Lyons *et al.*[13] demonstrated a decrease in the turn-on time of devices from ruthenium complexes upon blending with PEO. The turn-on time at an applied voltage of 6 V decreased from 2 minutes (pristine complex), down to less than 30 seconds for the films blended with PEO. The improvement was attributed to the increased ionic mobility upon blending with PEO. In contrast to previous work,[7,8] devices that were cooled below the glass transition temperature were found to exhibit symmetric current *vs*. voltage characteristics, indicating that ion concentration gradients can be readily erased. In addition, it was found that at room temperature, both the current and the radiance would continue to increase upon an application of a constant voltage. In contrast, steady-state was reached faster at low temperatures. This was attributed to the existence of two "modes" of charge transport: one which is slow and active at all temperatures, and another which is fast but only active to about −50 °C.

Handy *et al.*[14] demonstrated a simple scheme to decrease the turn-on time of devices based on a low molecular weight ruthenium complex. The turn-on time in these devices was found to be 2 minutes at 5 V, but upwards of 20 minutes at lower voltages. The turn-on time was decreased by the use of a pulsed biasing technique (Fig. 5). A short pulse at a higher voltage was

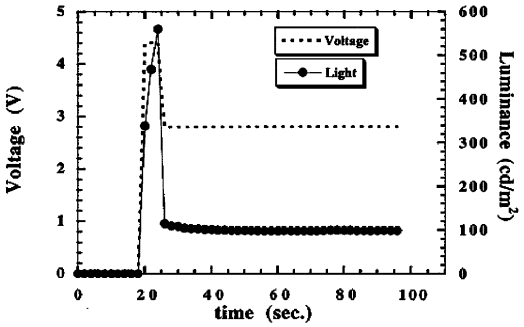

Fig. 5 Light output as a function of time and applied voltage. An initial voltage pulse of 4.4 V was applied, followed by operation at 2.8 V. From Ref. 14.

used to turn the device on, followed by a lower voltage that was used to drive the device for extended times, where the decay of the radiance with time was slower (more on that in the lifetime section).

The effect of various ligands on the turn-on time was also discussed in the same publication, where it was shown that complex, bulky ligands lead to longer turn-on times. The scaling of the turn-on time with film thickness was found to be different for materials with different ligands.

Very fast turn-on was reported by Gao and Bard[16] in ITO/$[Ru(bpy)_3]^{2+}(ClO_4^-)_2$/Ga:In devices. These devices reached their maximum radiance within 1–2 s at just 3 V. This was an improvement compared to devices based on $[Ru(bpy)_3]^{2+}(PF_6^-)_2$, which, at 3 V, showed a turn-on time exceeding 10 min.[14] Rudmann *et al.*,[20] reported a faster turn-on in devices from $[Ru(bpy)_3]^{2+}$ and similar complexes by using smaller counter ions. The time to reach 50% of maximum radiance in devices with BF_4^- and PF_6^- counter ions were <1 s and several minutes, respectively.

Buda *et al.*[21] considered the effects of environment on turn-on time. They observed that devices prepared in a dry box showed longer response times than devices prepared under ambient conditions. Furthermore, the difference between dry box and ambient was greater for small ions. For BF_4^- the difference was several orders of magnitude, whereas for AsF_6^- the difference was only a factor of 3–4. The results were attributed to changes in the counter ion mobility upon exposure to moisture. A solvation shell is generated around the counter ions by absorbed water, with the effect being greater for smaller ions because of the higher charge density.[27]

Leprêtre *et al.*[25] investigated the turn-on time of devices based on blends of a binuclear ruthenium complex with a lithium salt/crown ether electrolyte. For blends containing 50%, 66% and 75% wt. electrolyte, the turn-on times were up to 45 min, 20–30 min and 2 min, respectively. The decrease in the

turn-on time was associated with an increase in the ionic conductivity of the blends. The turn-on time decreased when anions with larger charge delocalization were used, which was attributed to increased ionic conductivity. Finally, coating the ITO with a conducting polymer was found to increase the turn-on times, attributed to the increased resistance of the electrode.

Barron *et al.*[29] reported on the transient behaviour of devices from polyamidoamine dendrimers containing pendant $[Ru(bpy)_3]^{2+}$ groups. Both the ionic and the electronic mobilities were found to decrease with dendrimer generation, as manifested by the increase of the turn-on time and the decrease of the steady-state current, respectively. Of note is the fact that by tuning the dynamic response of the material, the various regimes in the transient behaviour of the current were observed, as predicted by theory.[30]

Colour

The demonstration of multiple colours has so far received little attention, despite the fact that red, green and blue are required for applications in full colour displays and lighting. The majority of electroluminescent devices based on transition metal complexes reported thus far exhibit orange-red emission, with emission spectra having a maximum wavelength λ_{max} between 600 and 650 nm.

Some effort has been focused towards achieving saturated red colour. Handy *et al.*[14] demonstrated that attachment of ester groups to the ligands of $[Ru(bpy)_3]^{2+}$ increases λ_{max} to 690 nm. Similarly, Gao and Bard[16] demonstrated electroluminescent devices with λ_{max} of 690 nm by replacing one of the ligands in $[Ru(bpy)_3]^{2+}$ with $bpy(COOC_{12}H_{25})_2$.

Of note is the work of Welter *et al.*,[34] who reported devices based on a poly(*p*-phenylene vinylene) (PPV) derivative doped with a binuclear ruthenium complex. Under forward bias, these devices emit red light from the ruthenium complex, $[Ru(ph_4)Ru]^{4+}$, which consists of two $Ru(bpy)_3^{2+}$ units and four *p*-phenylene units as spacers. Under reverse bias, the devices emitted green light from the PPV. Asymmetric charge injection was proposed as a reason for the colour change upon the direction of the applied field.

Recently, Slinker *et al.*[26] reported devices based on $[Ir(ppy)_2(dtb\text{-}bpy)]^+(PF_6^-)$. These devices not only exhibited yellow emission (λ_{max} = 560 nm) under forward bias (Fig. 6), marking

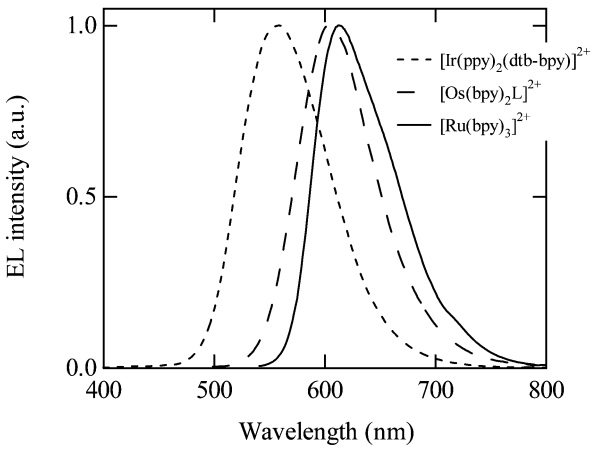

Fig. 6 Electroluminescence spectra from devices with ruthenium, osmium and iridium complexes under forward bias. ITO and Au where used as electrodes.

the first device based exclusively on a transition metal complex to emit at wavelengths below orange-red, but also exhibited a different colour (λ_{max} = 590 nm) when driven in reverse bias.

Lifetime

The lifetime of the electroluminescent devices under operating conditions, as well as their lifetime under storage are important figures of merit. Some attention has been paid to understanding the factors that control the lifetime of transition metal complex-based devices under operating conditions. Results are usually expressed by means of the half-life time, $t_{1/2}$, which indicates the time it takes for the radiance to decay to half of its maximum value under constant voltage driving conditions. The lifetime is limited by degradation processes such as oxidation of the metal electrodes or decomposition of the complex. Since lifetime is strongly affected by the environment in which the devices are operated, it is difficult to compare data among different groups. In this section we outline trends that have been observed in the device lifetimes.

Maness *et al.*[7,8] were the first to consider the lifetime of transition metal complex devices. They noticed that the degradation of the radiance emitted from a device based on a polymeric ruthenium complex was faster at higher applied voltages. The reduction of $[Ru(bpy)_3]^+$ species to $[Ru(bpy)_3]^0$ was cited as the reason for this degradation. The decay of diode-like behaviour over time was also studied in devices with frozen-in concentration gradients.

Elliott *et al.*[10] explored how the lifetime changed with device type. They found that planar-type devices made with inter-digitated arrays had a considerably shorter lifetime than sandwich-type devices.

Handy *et al.*[14] reported that the lifetime of devices based on $[Ru(bpy)_3]^{2+}(PF_6^-)_2$ and similar complexes was strongly linked to the applied voltage. For example, in one of these complexes, $t_{1/2}$ decreased from 2 hours to 5 min when the voltage was increased from 3 V to 5 V. The lifetime was found to be affected by the ligand. By varying the ligand, complexes with $t_{1/2}$ of 30 hours and 240 hours at 3 V were reported.

Rudmann and Rubner[17] showed that driving the devices under a 50% duty cycle improved lifetime. It was suggested that the reason for the improved stability was a change in the distribution of the counter ions compared to that under dc driving. In the same paper, they reported on the effects on the lifetime of using a low molecular weight ruthenium complex in PMMA, PC, and PS. It was found that $t_{1/2}$ varied from 700 h in the pristine film, to 500 h in the PC blend, to 900 h in the PPMA blend, to 1100 h in the PS blend. The differences were attributed to the quality of the film, suggesting that pinholes are a source of degradation. Furthermore, it was noted that devices with Al cathodes exhibited degradation upon storage in the off state. In contrast, devices with Ag cathodes were found to be stable upon storage in a dry box.

Crystalline $[Ru(bpy)_3]^{2+}(ClO_4^-)_2$ films fabricated by Liu and Bard[19] showed no degradation in performance over the course of 74 h of continuous operation at 3.5 V. This represented a considerable improvement compared to the lifetime of devices based on amorphous films of the same complex.[16]

The influence of the counter ion on the lifetime of low molecular weight ruthenium complex devices was studied by Rudmann *et al.*[20] Results showed that larger ions lead to longer device lifetimes, while smaller more mobile ions lead to shorter lifetimes. As a result, a trade-off between the turn-on time and the lifetime was observed.

The degradation of devices with Al cathodes was studied extensively by Rudmann *et al.*[22] using a combination of X-ray photoelectron spectroscopy and secondary ion mass spectroscopy (Fig. 7). It was found that degradation of these devices was

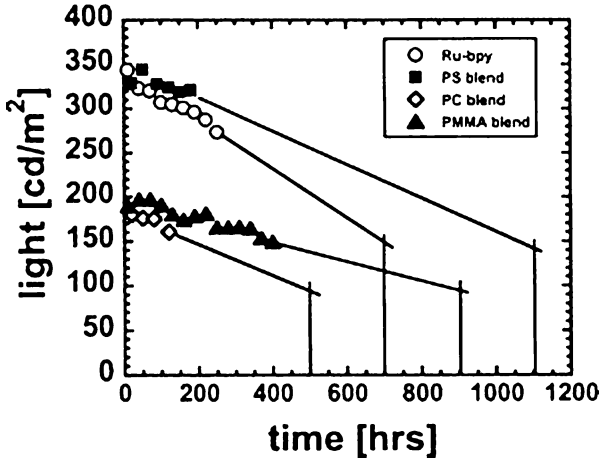

Fig. 7 Light emission *vs.* time of pristine and blend devices with PMMA, PC and PS. All blend devices contain about 25% vol. of polymer. All devices were operated at 5 V and 50% duty cycle at 1 kHz. The lines are extrapolations to determine $t_{1/2}$. From Ref. 17.

the result of a redox reaction between the metal and $[Ru(bpy)_3]^{2+}(PF_6^-)_2$.

Gao and Bard[23] studied the degradation of devices based on low molecular weight ruthenium and osmium complexes by systematically varying the electrodes. Devices with various anodes (ITO, antimony-doped tin oxide, Au), and various cathodes (Ga:In, Ga:Sn, Bi:In:Pt:Sn, Hg, Al) showed similar lifetimes, indicating that the degradation arises from the complex. By comparing the optical absorption spectrum of devices before and after operation, changes that were consistent with the build-up of an emission quencher were noticed. $[Os(bpy)_3]^{2+}(PF_6^-)_2$ devices were found to exhibit a longer lifetime than comparable devices made with $[Ru(bpy)_3]^{2+}(PF_6^-)_2$.

Bernhard *et al.*[24] used air stable electrodes such as ITO and Au electrodes to make devices with $[Ru(bpy)_3]^{2+}(PF_6^-)_2$. The device lifetime was independent of the polarity of the applied voltage (Fig. 4), indicating that degradation is associated with a reduction of the photoluminescence yield of the ruthenium complex over time, rather than a change in the injection or transport of carriers.

Leprêtre *et al.*[25] found that the addition of lithium salts in ruthenium-based devices decreased their lifetime. This was attributed to a fabrication environment that was unprotected from water and oxygen, and possibly the gradual degradation of the anion. Coating the ITO anode with a conducting polymer layer was found to increase lifetime. This was attributed to a combined effect of slowing down the release of oxygen and indium from ITO into the organometallic film and of planarisation of the electrode surface (which decreases the occurrence of microscopic shorts).

One of the most thorough investigations of device degradation was reported by Kalyuzhny *et al.*[27] Devices from $[Ru(bpy)_3]^{2+}(BF_4^-)_2$ films were prepared under an inert atmosphere, then tested in and out of a glove box. It was found that unipolar carrier injection led to no degradation, indicating that degradation requires the formation of the $[Ru(bpy)_3]^{2+*}$ species. Moreover, it was found that exposure to the ambient has a negative effect on device stability and that degradation is potentially the result of some first order irreversible reaction between a charged state of the complex and oxygen or moisture. By monitoring the photoluminescence alongside the electroluminescence in planar devices, it was determined that degradation occurs in a relatively thin region of the organic film close to the cathode. As a result it was proposed that degradation was the result of the generation of a quencher. It is noted that $[Ru(bpy)_2(H_2O)_2]^{2+}$ in small amounts has been known to considerably decrease emission efficiency and may be the quencher in this system.

Outlook

Electroluminescent devices based on transition metal complexes offer several attractive features. Due to the multifunctional nature of these materials, efficient devices can be fabricated by simply sandwiching a single, solution-processed layer between two metal electrodes. The availability of mobile ions enables the use of air-stable electrodes, which is a big advantage compared to traditional OLEDs. Numerous studies of their electrochemical and spectroscopic properties provide an extensive knowledge basis that can help understand and optimise device performance.

Devices with ohmic contacts can be easily fabricated due to the enhancement in charge injection brought by the mobile ions. In these devices, the quantum efficiency is not limited by the magnitude and the balance of the electron and hole currents, but solely by the photoluminescence yield of the complex. This limit has already been reached in devices based on $[Ru(bpy)_3]^{2+}$ and a few other similar complexes.[24] However, even more efficient devices can be expected by using complexes with a higher yield of photoluminescence: For example, a ruthenium complex that exhibits a solution photoluminescence yield of 40% (compared to 6% for $[Ru(bpy)_3]^{2+}$, in solution[24]) has been reported.[35] Careful studies where the efficiency of electroluminescence is compared to the photoluminescence yield of the film are important to understand bottlenecks in device efficiency and should be pursued whenever possible. In addition to using complexes with more efficient emission, engineering of the device can be performed to increase the fraction of extracted photons.[36,37]

The long turn-on time of these devices remains a challenging issue. Although turn-on times of the order of a second have been demonstrated in some devices, their response remains too slow for most display applications, where video rate is required. Clearly, more research needs to be done to better understand the ultimate limits of the turn-on time in these materials. To this extent, careful experiments seeking a quantitative understanding of the relationship between ionic conductivity and the turn-on should be performed. The use of pre-biasing schemes, as well as the formation of counter ion concentration gradients are promising ways to decrease the turn-on time.

The issue of colour tunability has not yet been addressed. The vast majority of complexes reported in literature photoluminesce in the orange-red part of the spectrum. It should be noted, however, that a few complexes with photoluminescence in the blue part of the spectrum have been reported[38,39] and it is a matter of time until they are tested in electroluminescent devices. It remains to be seen whether efficient injection can still take place from air-stable electrodes in materials with a large HOMO/LUMO gap.

As far as lifetime is concerned, devices based on transition metal complexes are at an advantage compared to OLEDs. Transition metal complexes are intrinsically more stable towards redox reactions compared to most organic semiconductors. In addition, due to the fact that air-stable electrodes can be used, oxidation of the metal is no longer a concern. Encapsulation technologies developed for OLEDs can be directly applied to devices from these materials, if necessary. Of concern is the trade-off between the lifetime and the turn-on time, observed by Rudmann *et al.*[20] and by Leprêtre *et al.*[25] It is not clear at this moment whether this trade-off is related to the nature of the specific counter ions used in these devices or it represents a general trend. Further research is needed to address this issue.

Perhaps the first commercial endeavour of these devices will be in applications where turn-on time and colour are not very important, while low cost (hence simple fabrication) and low power consumption (hence high efficiency) are required. Monochromatic alphanumeric displays and backlights (such as the one shown in Fig. 8) fall in this category. With further

Fig. 8 Electroluminescent device based on $[Ru(bpy)_3]^{2+}$. Photo courtesy of Professor Michael Rubner, MIT.

progress on the turn-on time and the colour tunability, applications in full colour displays and lighting will be within reach.

Acknowledgement

This work was supported by the National Science Foundation (Career Award DMR-0094047) and by the Cornell Center for Materials Research (CCMR), a Materials Research Science and Engineering Center of the National Science Foundation (DMR-9632275).

Notes and references

1 D. M. Roundhill, *Photochemistry and Photophysics of Metal Complexes*, Plenum, New York 1994.
2 N. E. Tokel and A. J. Bard, *J. Am. Chem. Soc.*, 1972, **94**, 2862–2863.
3 J. C. Scott and G. G. Malliaras, in *Conjugated Polymers*, (Eds: G. Hadziioannou, P. F. van Hutten), Wiley-VCH, New York, 1999; Ch. 13.
4 K. Kalyanasundaram, *Photochemistry of Polypyridine and Porphyrin Complexes*, Academic Press, London, 1992.
5 Q. B. Pei, G. Yu, C. Zhang and A. J. Heeger, *Science*, 1995, **269**, 1086–1088.
6 J. K. Lee, D. S. Yoo, E. S. Handy and M. F. Rubner, *Appl. Phys. Lett.*, 1996, **69**, 1686–1688.
7 K. M. Maness, R. H. Terrill, T. J. Meyer, R. W. Murray and R. M. Wightman, *J. Am. Chem. Soc.*, 1996, **118**, 10609–10616.
8 K. M. Maness, H. Masui, R. M. Wightman and R. W. Murray, *J. Am. Chem. Soc.*, 1997, **119**, 3987–3993.
9 J. K. Lee, D. S. Yoo and M. F. Rubner, *Chem. Mater.*, 1997, **9**, 1710–1712.
10 C. M. Elliott, F. Pichot, C. J. Bloom and L. S. Rider, *J. Am. Chem. Soc.*, 1998, **120**, 6781–6784.
11 A. P. Wu, J. K. Lee and M. F. Rubner, *Thin Solid Films*, 1998, **329**, 663–667.
12 X. Gong, P. K. Ng and W. K. Chan, *Adv. Mater.*, 1998, **10**, 1337–1340.
13 C. H. Lyons, E. D. Abbas, J. K. Lee and M. F. Rubner, *J. Am. Chem. Soc.*, 1998, **120**, 12100–12107.
14 E. S. Handy, A. J. Pal and M. F. Rubner, *J. Am. Chem. Soc.*, 1999, **121**, 3525–3528.
15 A. P. Wu, D. S. Yoo, J. K. Lee and M. F. Rubner, *J. Am. Chem. Soc.*, 1999, **121**, 4883–4891.
16 F. G. Gao and A. J. Bard, *J. Am. Chem. Soc.*, 2000, **122**, 7426–7427.
17 H. Rudmann and M. F. Rubner, *J. Appl. Phys.*, 2001, **90**, 4338–4345.
18 S. Bernhard, X. Gao, G. G. Malliaras and H. D. Abruña, *Adv. Mater.*, 2002, **14**, 433–436.
19 C. Y. Liu and A. J. Bard, *J. Am. Chem. Soc.*, 2002, **124**, 4190–4191.
20 H. Rudmann, S. Shimada and M. F. Rubner, *J. Am. Chem. Soc.*, 2002, **124**, 4918–4921.
21 M. Buda, G. Kalyuzhny and A. J. Bard, *J. Am. Chem. Soc.*, 2002, **124**, 6090–6098.
22 H. Rudmann, S. Shimada, M. F. Rubner, D. W. Oblas and J. E. Whitten, *J. Appl. Phys.*, 2002, **92**, 1576–1581.
23 F. G. Gao and A. J. Bard, *Chem. Mater.*, 2002, **14**, 3465–3470.
24 S. Bernhard, J. A. Barron, P. L. Houston, H. D. Abruña, J. L. Ruglovksy, X. Gao and G. G. Malliaras, *J. Am. Chem. Soc.*, 2002, **124**, 13624–13628.
25 J.-C. Leprêtre, A. Deronzier and O. Stéphan, *Synth. Met.*, 2002, **131**, 175–183.
26 J. Slinker, A. Gorodetsky, S. Bernhard and G. G. Malliaras, *J. Am. Chem. Soc.*, 2003 (in press).
27 G. Kalyuzhny, M. Buda, J. McNeill, P. Barbara and A. J. Bard, *J. Am. Chem. Soc.*, 2003, **125**, 6272–6283.
28 K. W. Lee, J. Slinker, A. A. Gorodetsky, S. Flores-Torres, H. D. Abruña, P. L. Houston and G. G. Malliaras, *Physical Chemistry and Chemical Physics*, 2003, **5**, 2706–2709.
29 J. A. Barron, S. Bernhard, P. L. Houston, H. D. Abruña, J. Ruglovsky and G. G. Malliaras, *J. Phys. Chem.*, 2003 (in press).
30 J. C. deMello, N. Tessler, S. C. Graham and R. H. Friend, *Phys. Rev. B*, 1998, **57**, 12951–12963.
31 G. G. Malliaras and J. C. Scott, *J. Appl. Phys.*, 1998, **83**, 5399–5403.
32 F.-R. F. Fan and A. J. Bard, *J. Phys. Chem. B.*, 2003, **107**, 1781–1787.
33 H. Rudmann, S. Shimada and M. F. Rubner, *J. Appl. Phys.*, 2003, **94**, 115–122.
34 S. Welter, K. Brunner, J. W. Hofstraat and L. De Cola, *Nature*, 2003, **421**, 54–57.
35 P. C. Alford, M. J. Cook, A. P. Lewis, G. S. G. McAulifee, V. Skarda, A. J. Thompson, J. L. Glasper and D. J. Robbins, *J. Chem. Soc.Perkin Trans.2*, 1985, 705–709.
36 T. Yamasaki, K. Sekumioka and T. Tsutsui, *Appl. Phys. Lett.*, 2000, **76**, 1243–1245.
37 C. F. Madigan, M.-H. Lu and J. C. Sturm, *Appl. Phys. Lett.*, 2000, **76**, 1650–1652.
38 M. K. DeArmond, M. C. Carlin and W. L. Huang, *Inorg. Chem.*, 1980, **19**, 62–67.
39 G. A. Crosby and W. H. Elfring Jr., *J. Phys. Chem.*, 1976, **80**, 2206–2211.